


ORIGINAL ARTICLE

Cyclophilin D as a potential therapeutic target of liver ischemia/reperfusion injury by mediating crosstalk between apoptosis and autophagy

Mengjiao Yang^{1,2,3} | Zhihui Wang^{1,2,3} | Jin Xie² | Md. Reyad-ul-Ferdous^{2,3,4} | Siying Li^{3,5}  | Yongfeng Song^{1,2,3,5}

¹Department of Endocrinology, Shandong Provincial Hospital Affiliated to Shandong First Medical University, Jinan, Shandong, China

²Shandong Key Laboratory of Endocrinology and Lipid Metabolism, Jinan, Shandong, China

³Shandong Institute of Endocrine and Metabolic Diseases, Jinan, Shandong, China

⁴Department of Endocrinology, Shandong Provincial Hospital, Cheeloo College of Medicine, Shandong University, Jinan, Shandong, China

⁵Department of Endocrinology and Metabolism, Central Hospital Affiliated to Shandong First Medical University, Jinan, Shandong, China

Correspondence

Yongfeng Song, Department of Endocrinology, Shandong Provincial Hospital Affiliated to Shandong First Medical University, 324 Jing 5 Rd, Huaiyin District, Jinan, Shandong 250021, China.

Email: syf198506@163.com

Siying Li, Shandong Institute of Endocrine and Metabolic Diseases, Jinan, Shandong 250021, China.

Email: lisiying@sdfmu.edu.cn

Edited by Yi Cui

Funding information

Independently cultivates innovation team program of Jinan, China, Grant/Award Number: 2021GXRC048; Shandong Provincial Natural Science Foundation, Grant/Award Number: ZR2020ZD14; National Natural Science Foundation of China, Grant/Award Number: 82270922; National Key Research and Development Program of China, Grant/Award Number: 2022YFA0806100

Abstract

Background: Liver ischemia/reperfusion (I/R) injury is a complex and multifactorial pathophysiological process. It is well recognized that the membrane permeability transition pore (mPTP) opening of mitochondria plays a crucial role in cell death after I/R injury. Cyclophilin D (CypD) is a critical positive regulator of mPTP. However, the effect of CypD on the pathogenesis of liver I/R injury and whether CypD is a potential therapeutic target are still unclear.

Methods: We constructed liver-specific CypD knockout and AAV8-peptidyl prolyl isomerase F (PPIF) overexpression mice. Then, a 70% liver I/R injury model was established in mice, with 90 min of ischemia and 6 h of reperfusion. The liver function was detected by the level of serum glutamic pyruvic transaminase (alanine transaminase) and glutamic oxaloacetic transaminase (aspartate aminotransferase), the liver damage score and degree of necrosis were measured by hematoxylin and eosin (H&E) staining of liver tissues. Reactive oxygen species (ROS) staining, apoptosis, and autophagy-related molecules were used to detect apoptosis and autophagy during liver I/R.

Results: The liver-specific knockout of CypD alleviated necrosis and dysfunction in liver I/R injury, by reducing the excessive production of ROS, and inhibiting cell apoptosis and autophagy. On the contrary, overexpression of CypD exacerbated I/R-induced liver damage.

Conclusion: We found that the downregulation of CypD expression alleviated liver I/R injury by reducing apoptosis and autophagy through caspase-3/Beclin1 crosstalk; in contrast, the upregulation of CypD expression aggravated liver I/R injury. Therefore, interfering with the expression of CypD seems to be a promising treatment for liver I/R injury.

KEYWORDS

apoptosis, autophagy, cyclophilin D, ischemia/reperfusion, necrosis, reactive oxygen species

Key points

- A liver-specific cyclophilin D (CypD) knockout mouse model was established, and we first reported the effect of liver-specific CypD knockout on liver ischemia/reperfusion in mice.
- This study adds AAV8-peptidyl prolyl isomerase F overexpression models.

This is an open access article under the terms of the Creative Commons Attribution-NonCommercial-NoDerivs License, which permits use and distribution in any medium, provided the original work is properly cited, the use is non-commercial and no modifications or adaptations are made.

© 2023 The Authors. *Chronic Diseases and Translational Medicine* published by John Wiley & Sons Ltd on behalf of Chinese Medical Association.

1 | INTRODUCTION

During liver transplants, hepatectomy, and hemorrhagic shock, liver ischemia/reperfusion (I/R) injury is one of the leading causes of liver dysfunction and even mortality.^{1,2} Generally, I/R can be divided into two types: warm I/R or cold I/R. Warm I/R injury can occur in cases of hepatectomy, hemorrhagic shock, cardiac arrest, or hepatic sinus obstruction syndrome.³ This study only discusses warm I/R. Ischemia-induced hypoxia, ATP consumption, and oxygen depletion lead to hepatocyte death, while reperfusion induces immune cell infiltration and excessive reactive oxygen species (ROS) production, exacerbating hepatocellular injury.^{4,5} The vicious cycle of I/R, which promotes the development of liver injury, is generally considered to be the result of excessive production of ROS, calcium overload, endoplasmic reticulum stress, and mitochondrial damage.⁶ Therefore, the identification of promising therapeutic strategies is necessary for alleviating liver I/R injury.

Mitochondria are the key target or origin of tissue damage, especially in I/R injury.⁷ Mitochondrial damage is a common result of liver I/R, accompanied by mitochondrial cristae breakage and disappearance, mitochondrial membrane potential decrease, and mitochondrial permeability transition pore (mPTP) activation.⁸⁻¹⁰

mPTP opening plays a crucial role in the mechanism of cell death after I/R injury.^{11,12} In the mitochondrial matrix, cyclophilin D (CypD) is an isomer of peptidyl prolyl isomerase F (PPIF) and maintains mitochondrial function by regulating mitochondrial permeability to various stimuli together with Pi.¹³ CypD inhibition has been shown to have potential benefits in neurological diseases such as Alzheimer's disease, Parkinson's disease, and cerebral ischemia.^{14,15} CypD knockout also attenuated mitochondrial perturbation and inhibited the progression of early nonalcoholic steatohepatitis (NASH) by ameliorating steatosis and inflammatory symptoms in our previous study.¹⁶ However, the effects of CypD on the pathogenesis of liver I/R injury and the potential therapeutic value of CypD remain to be explored.

Overall, we focused on the critical role of CypD in liver I/R injury. The purpose of this research is to clarify the mechanism by which CypD is involved in complex forms of cell death, including necrosis, apoptosis, and autophagy. We hypothesized that targeting CypD may be a potential therapeutic strategy for liver protection in I/R injury.

2 | MATERIALS AND METHODS

2.1 | Animal details

The Jackson Laboratory provided mice (C57BL/6J) carrying a conditionally expressed CypD allele (CypD^{fl/fl}). Using CypD^{fl/fl} mice mated with albumin-Cre mice, liver-specific CypD knockout (CypD LKO) mice were generated. For the

CypD LKO mice, CypD^{fl/fl} littermates were used as controls. Supporting Information: Table 1 shows the primers for genotypic identification of CypD mice.

Mouse models of CypD overexpression were established using AAV8-PPIF (43955; Shanghai GeneTech Company Limited). Briefly, male C57BL/6 mice were obtained from Beijing Vital River Laboratory Animal Technology Co. Ltd. In addition, AAV8-PPIF (CypD overexpression adeno-associated virus) and AAV8-Con (con adeno-associated virus) were dissolved in sterile phosphate buffered saline (PBS) at a concentration of 1×10^{11} vector genomes and were injected through the caudal vein of mice at 8 weeks. After 1 month, the mice were killed for subsequent experiments.

All mice were housed in a specific pathogen-free (SPF) room in a constant temperature-controlled environment with a 12-h light/dark cycle. Before surgery, mice were fasted for 8 h and allowed to drink freely. The Research Ethics Committee of Shandong Provincial Hospital approved all procedures (No. 2022-047).

2.2 | Establishment of the hepatic I/R model

The standard protocol for establishing 70% liver warm I/R injury models in mice has already been described.¹⁷ A midline incision was created to open the abdominal cavity among the left lateral and median lobes of the liver, and an atraumatic vascular clip (Shanghai Medical Equipment (Group) Co., Ltd. Surgical Equipment Factory) was placed across the bile duct, portal vein, and hepatic artery to interrupt 70% of the blood supplied to the liver. Atraumatic vascular clamping was removed after 90 min of ischemia. After the atraumatic vascular clip was removed, reperfusion was resumed for 6 h. In the sham operation group, the same surgery was performed, but no atraumatic vascular clips were used. During ischemia, all mice were placed on a 37°C thermostatic pad to maintain body temperature. Finally, the mice were anesthetized with pentobarbital sodium (100 μ L/10 g, i.p.) and killed to obtain liver tissue and serum samples.

Group design was as follows: CypD^{fl/fl} mice and CypD LKO mice were divided into two groups (seven mice per group) according to whether they had undergone ischemia/reperfusion surgery. The grouping of AAV8-PPIF mice and AAV8-Con mice was the same as described above.

2.3 | Serum biochemistry analysis

At 4°C, blood samples from each group of mice were centrifuged for 15 min at 3000 rpm/min, and automatic biochemical analyzers (Mindray) were used to analyze the glutamic pyruvic transaminase (alanine transaminase [ALT]) and glutamic oxaloacetic transaminase (aspartate aminotransferase [AST]) levels in the upper serum.

2.4 | RNA sequencing (RNA-seq)

Novogene Technology conducted all transcriptome analyses. The RNA Nano 6000 analysis kit of the Bioanalyzer 2100 system (Agilent Technologies) was used to evaluate the quality of RNA and identify the integrity of RNA. RNA samples were prepared with total RNA as input material. In brief, the mRNA was purified from the total RNA by using magnetic beads connected with polyT oligonucleotides. The AMPure XP system was used to screen 370–420 bp template DNA from purified fragments. For polymerase chain reaction (PCR) amplification, Phusion high-fidelity DNA polymerase, PCR primers, and target primers were used. Finally, the PCR products were purified.

2.5 | Histological hematoxylin and eosin (H&E) staining, immunohistochemistry (IHC), and immunofluorescence

A 4% paraformaldehyde fixation for over 24 h was followed by paraffin embedding of liver tissue samples. Liver histopathological changes were observed under an optical microscope (TissueFAXS Spectra, TissueGnostics) after sectioning (5 mm thick) and staining with H&E.

IHC staining was performed on paraffin-embedded liver tissue slides after dewaxing, rehydrating, antigen retrieval, and incubation with primary antibodies against Beclin1 (ab217179; Abcam PLC) and translocase of outer mitochondrial membrane 20 (TOMM20) (ab186735; Abcam PLC) overnight at 4°C. Then, the cells were incubated with the secondary antibody for 1 h at 37°C, and the nuclei were counterstained with hematoxylin. An optical microscope was used to observe and capture images of the sections.

For immunofluorescence, frozen mouse liver sections were fixed with 4% paraformaldehyde, permeabilized with 0.5% Triton X-100 in PBS, and blocked with 5% goat serum before incubation with mouse anticlaved caspase-3 (9664; Cell Signaling Technology, Inc.) overnight at 4°C. Then, the cells were incubated with the secondary antibody for 1 h at 37°C, and nuclei were counterstained with 4',6-diamidino-2-phenylindole (DAPI) (A11034; Invitrogen). Finally, images were captured under a fluorescence microscope (TissueFAXS Spectra; TissueGnostics).

2.6 | Detection of ROS production in liver tissues

We used the BBoxiProbe[®] O13 kit (BB-470513; BestBio) to determine ROS levels in liver tissues. BBoxiProbe[®] O13 is a fluorescent probe for cell membrane permeability. It is specifically oxidized by ROS to generate red fluorescent substances. The red fluorescence intensity is proportional to the level of ROS. In brief, frozen sections of liver tissues (10 μm thick) were prepared and

incubated with BBoxiProbe[®] O13 for 1 h in the dark at 37°C. Fluorescence microscopy was used to observe the sections at 610 nm wavelength after staining with DAPI.

2.7 | Transmission electron microscopy (TEM)

TEM was used to confirm and monitor autophagy, mitochondria, and the quantification of autophagic vacuoles. Liver tissue samples (1 mm³) were immediately fixed in 2.5% glutaraldehyde overnight at 4°C. The liver tissues were washed with PBS three times and fixed in 1% osmium tetroxide for 2 h at room temperature. A graded alcohol series was used to dehydrate fixed tissues, and then Epon resin was used to embed them. Sections (70 nm) were prepared and stained with uranyl acetate and lead citrate after the blocks were cured at 60°C for 48 h. Finally, the sections were analyzed and imaged under a TEM (JEOL-1200; Weiya Bio Co., Ltd.).

2.8 | TUNEL

In the liver sections, apoptosis was detected by terminal deoxynucleotidyl transferase dUTP nick-end labeling (TUNEL) assay as directed by the manufacturer (KGA7073; Jiangsu KeyGEN BioTECH Co. Ltd.). The apoptotic cells showed green fluorescence.

2.9 | Western blot analysis

Equal amounts of protein extracts were separated by 20% sodium dodecyl sulfate polyacrylamide gel electrophoresis (SDS-PAGE) and transferred to 0.22 μm or 0.45 μm polyvinylidene difluoride (PVDF) membranes. The membranes were blocked with 5% nonfat milk for 1 h at room temperature before being incubated with primary antibodies overnight at 4°C, which included antibodies against cyclophilin F (ab110324; Abcam PLC), Beclin1 (ab217179; Abcam PLC), TOMM20 (ab186735; Abcam PLC), caspase-3 (19677-1-AP; ProteinteCh Group, Inc.) and cleaved caspase-3 (9664; Cell Signaling Technology, Inc.). The next day, the secondary antibody was incubated for an hour with the corresponding horseradish peroxidase-conjugated mouse or rabbit antibody (1:5000). Immunoreactive proteins were then measured through an enhanced chemiluminescence detection system (GE AI680; General Electric Company).

2.10 | RNA isolation and quantitative real-time PCR (RT-PCR)

Total RNA was extracted from liver tissues using TRIzol reagent (R401-01; Nanjing Vazyme Biotech Co. Ltd.).

The concentration and purity of the RNA were determined using a Nanodrop spectrophotometer (ND-DIVEC; Gene Company Limited). Quantitative RT-PCR analyses were performed with the SYBR Green PCR Master Mix reagent kit (Q311-02, Nanjing Vazyme Biotech Co. Ltd.). A Roche 480 detection system was used to perform the quantitative PCR analysis, and the relative level of mRNA was analyzed using the $2^{-\Delta\Delta C_t}$ method. Supporting Information: Table 2 lists the primer sequences.

2.11 | Statistical analysis

All results are presented as the means \pm SEMs. We used GraphPad Prism version 8.3.0 (GraphPad Software) and evaluate the comparison between groups using one-way analysis of variance (ANOVA). Statistical significance was determined based on the p value, and a $p < 0.05$ was considered to indicate statistical significance.

3 | RESULTS

3.1 | The effect of CypD on hepatocyte damage caused by liver I/R

To explore the potential effect of CypD on hepatic I/R injury, liver-specific CypD knockout mice and AAV8-PPIF overexpression mice were generated. CypD knockout in mouse livers was confirmed by PCR/Western blot analysis (Figure 1A,B). Compared with the CypD^{fl/fl} I/R group, the impairment of liver function was alleviated in the CypD LKO I/R group. As shown in Figure 1C, CypD^{fl/fl} mice showed impaired liver function and obvious hepatocyte injury after liver I/R, such as hepatic lobular disorder and cell necrosis. Hepatic cellular injury and necrosis were significantly alleviated in the CypD LKO I/R group. In addition, serum AST and ALT levels were lower in the CypD LKO I/R group than in the CypD^{fl/fl} I/R group (Figure 1D,E). AAV8-PPIF overexpression was confirmed by PCR/Western blot analysis (Figure 1F,G). In contrast, AAV8-PPIF-treated mice exhibited severe liver injury, along with increased necrotic areas compared with AAV8-Con-treated mice (Figure 1H).

3.2 | CypD triggers ROS overproduction in liver I/R injury

Liver ischemia/reperfusion is characterized by excessive ROS production, which triggers mPTP activation, subsequent mitochondrial damage, and cell death. BBoxiProbe[®] O13 was used to test ROS production. As shown in Figure 2A, the red fluorescence in the CypD LKO I/R group was obviously diminished compared with that in the CypD^{fl/fl} I/R group. Similarly, we also observed that the AAV8-PPIF I/R group had significantly augmented red

fluorescence compared with the AAV8-Con I/R group (Figure 2B). These results indicated that CypD knockout could attenuate liver I/R-induced hepatocyte injury, necrosis, and ROS production in mice. However, CypD overexpression showed the opposite effects.

3.3 | CypD initiates hepatocyte apoptosis in liver I/R injury

Apoptosis is an essential physiological process to maintain tissue homeostasis, and apoptotic cells were detected by TUNEL staining. As shown in Figure 2C, there were a large number of positively stained cells in the CypD^{fl/fl} I/R group, while the number of positive cells was sharply reduced in the CypD LKO I/R group. In contrast, after ischemia/reperfusion surgery, immunofluorescence staining with cleaved caspase-3 increased in the AAV8-PPIF group compared with the AAV8-Con group (Figure 3C). We also observed that the number of positive cells in the AAV8-PPIF I/R group was enormously increased compared with that in the AAV8-Con I/R group with TUNEL staining (Figure 2D). These results showed that CypD knockout could alleviate apoptosis in the liver I/R injury model.

The induction and execution of apoptosis are regulated in an orderly way by a series of proteolytic caspase cascades under certain circumstances. Caspase-3 has been recognized as a predominant mediator of apoptosis. As shown in Figure 3B, compared with the CypD^{fl/fl} I/R group, cleaved caspase-3 decreased significantly in the CypD LKO I/R group. Similarly, immunofluorescence staining with cleaved caspase-3 also proved the above point of view (Figure 3A).

3.4 | CypD participates in autophagic cell death in hepatic I/R injury

Due to the complexity of liver ischemia/reperfusion-induced cell death and dysfunction, RNA-Seq was used to identify novel genes and transcription factors involved in CypD LKO I/R mice. Through Kyoto Encyclopedia of Genes and Genomes (KEGG) enrichment analysis, a significant difference in autophagy between the CypD^{fl/fl} I/R group and CypD LKO I/R group revealed an autophagy-related cell death pathway (Figure 4A,B). The formation of autophagosomes is a crucial process of autophagy. As shown in Figure 4C, mitochondrial swelling, mitochondrial cristae breakage and disappearance and an increase in lysosomes and autophagosomes were observed in the CypD^{fl/fl} I/R group. In comparison, the liver structure of the CypD LKO I/R group was still intact, and the number of lysosomes and autophagosomes was lower. These results indicated that CypD mediated autophagic cell death in liver I/R injury.

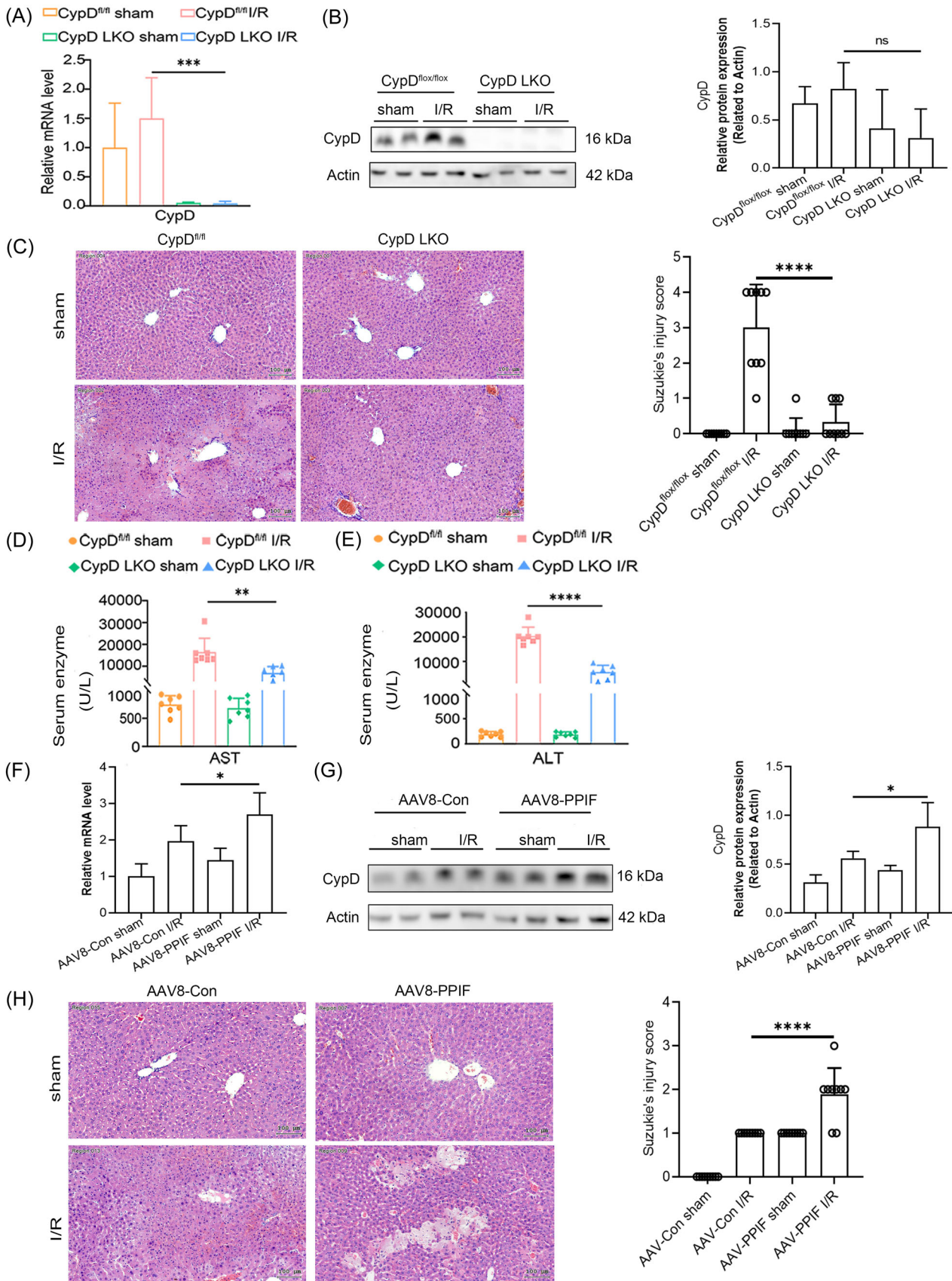


FIGURE 1 (See caption on next page)

It is well known that TOMM20 and Beclin1 play important roles in autophagy. TOMM20 is widely used to monitor mitochondrial mass during autophagy, and a decrease in its expression is considered a reduction in mitochondrial mass and upregulation of mitochondrial autophagy. As shown in Figure 5A,C, the expression of TOMM20 increased in the CypD LKO I/R group compared with the CypD^{fl/fl} I/R group. CypD overexpression decreased TOMM20 expression in the AAV8-PPIF I/R group compared with the AAV8-Con I/R group (Figure 5E). The autophagy-related protein Beclin1 is a mammalian gene that is positively related to autophagy and is important for the formation of autophagosomes. Consequently, the change in Beclin1 was examined. Compared with that in the CypD^{fl/fl} I/R group, the expression of Beclin1 in the CypD LKO I/R group decreased (Figure 5B,D). Additionally, IHC revealed upregulation of Beclin1 in the AAV8-PPIF I/R group compared with the AAV8-Con I/R group (Figure 5F).

4 | DISCUSSION

Necrosis, apoptosis, and autophagy are the three main types of programmed cell death in patients with I/R injury.³ At present, a few effective therapeutic strategies can be used to prevent or treat I/R-induced injury.¹⁸ The purpose of this research is to study the role of CypD in liver I/R injury from these aspects of cell death. In this study, liver-specific CypD knockout and overexpression were explored in vivo. We found that in liver I/R injury, the knockout of CypD can alleviate liver injury by reducing hepatocyte necrosis, apoptosis, and autophagy, and vice versa.

There are many mechanisms involved in I/R-induced injury. Oxygen loss and nutrient depletion during ischemia lead to ATP deficiency in parenchymal and nonparenchymal liver cells, which disrupts intracellular energy-dependent metabolic and transporting processes, leading to the accumulation of ROS.¹⁹ It has been reported that the opening of mPTP is the main cause of cell death caused by reperfusion injury, so it is an important target of cytoprotection.²⁰ During I/R injury, the opening of mPTP leads to the loss of membrane potential, ATP depletion, matrix swelling, uncoupling of oxidative phosphate, and overproduction of ROS, which ultimately leads to cell death.^{12,21,22} CypD is the major modulator of mPTP, which plays a crucial

role in maintaining the mitochondrial function of hepatocytes.²³ The upregulation of CypD can provoke the excessive opening of mPTP, which leads to the accumulation of damaged mitochondria.²⁴ As a result, abnormal CypD-mPTP axis activation has been implicated in the development of various diseases, such as ischemia/reperfusion injuries, aging, and neurodegenerative conditions.^{19,25,26} However, the specific knockout or overexpression of CypD in mouse liver I/R injury is still unclear. In our study, CypD overexpression resulted in more severe liver injury, mitochondrial destruction, and ROS production in I/R mice, but CypD deletion attenuated liver I/R injury in CypD LKO mice. These results demonstrated that hepatic CypD mediates mitochondria-dependent cell death in liver I/R injury.

It has been shown that the opening of mPTP increases mitochondrial membrane permeability and cell apoptosis.¹⁸ Therefore, blocking mPTP opening during the reperfusion phase of the liver can significantly reduce apoptosis after I/R-induced injury. Previous studies have shown that cyclosporin A, an inhibitor of CypD, can improve the apoptosis induced by warm ischemia-reperfusion injury in rats.²⁷ TUNEL staining showed that liver CypD knockout exhibited an obvious effect in reducing hepatocyte apoptosis; conversely, CypD overexpression increased hepatocyte apoptosis. The activation and function of caspases, which are involved in the delicate caspase-cascade system, is vital in the process of apoptotic signal conduction. It has been demonstrated that mPTP induction activates caspase-3 activity in myofiber atrophy.²⁸ Caspase-3 activity was blocked in liver-specific CypD knockout mice in the I/R model, as indicated by cleaved caspase-3 expression. Therefore, CypD may contribute to hepatocyte apoptosis in a caspase-3-dependent manner in liver I/R injury.

Autophagy is a conservative cell protection process that can maintain cell homeostasis.¹⁷ Autophagy involves the formation of the double membrane structure of autophagosomes. Cargoes enveloped by autophagosomes are transported directly to autolysosomes, where they are degraded by lysosomal enzymes.^{29,30} Autophagy is usually considered a cell protection mechanism; however, excessive autophagy can lead to cell death. In addition, many previous studies have shown that the upregulation³¹ or downregulation³² of autophagy has a protective effect on the attenuation of liver I/R injury according to specific

FIGURE 1 The effect of CypD on liver damage caused by liver I/R injury. (A) The mRNA levels of CypD in liver-specific CypD knockout live tissue ($n = 3$ per group). (B) Protein expression of CypD in liver-specific CypD knockout live tissue. (C) H&E staining of CypD^{fl/fl} group and CypD LKO group mice. Scale bar = 100 μ m ($n = 3$ per group). (D) Serum AST concentration ($n = 7$ per group). (E) Serum ALT concentration ($n = 7$ per group). (F) The mRNA levels of CypD in the livers of AAV8-PPIF-overexpressing mice ($n = 3$ per group). (G) Protein expression of CypD in the livers of AAV8-PPIF-overexpressing mice. (H) H&E staining of AAV8-Con group and AAV8-PPIF group mice ($n = 3$ per group). * $p < 0.05$; ** $p < 0.01$; *** $p < 0.001$. ALT, alanine transaminase; AST, aspartate aminotransferase; CypD, cyclophilin D; CypD LKO, liver-specific CypD knockout; H&E, hematoxylin and eosin; I/R, ischemia/reperfusion; PPIF, peptidyl prolyl isomerase F.

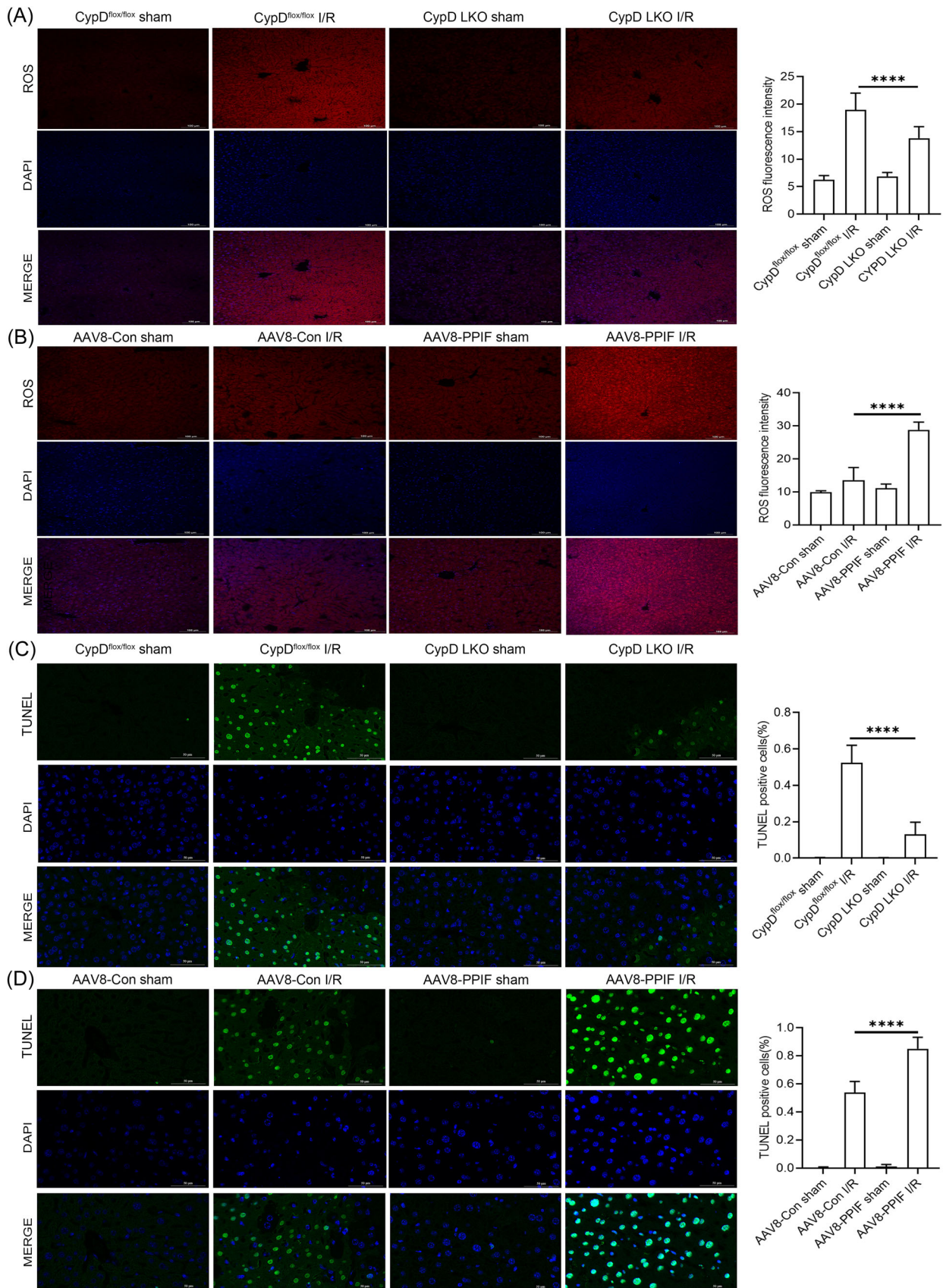


FIGURE 2 (See caption on next page)

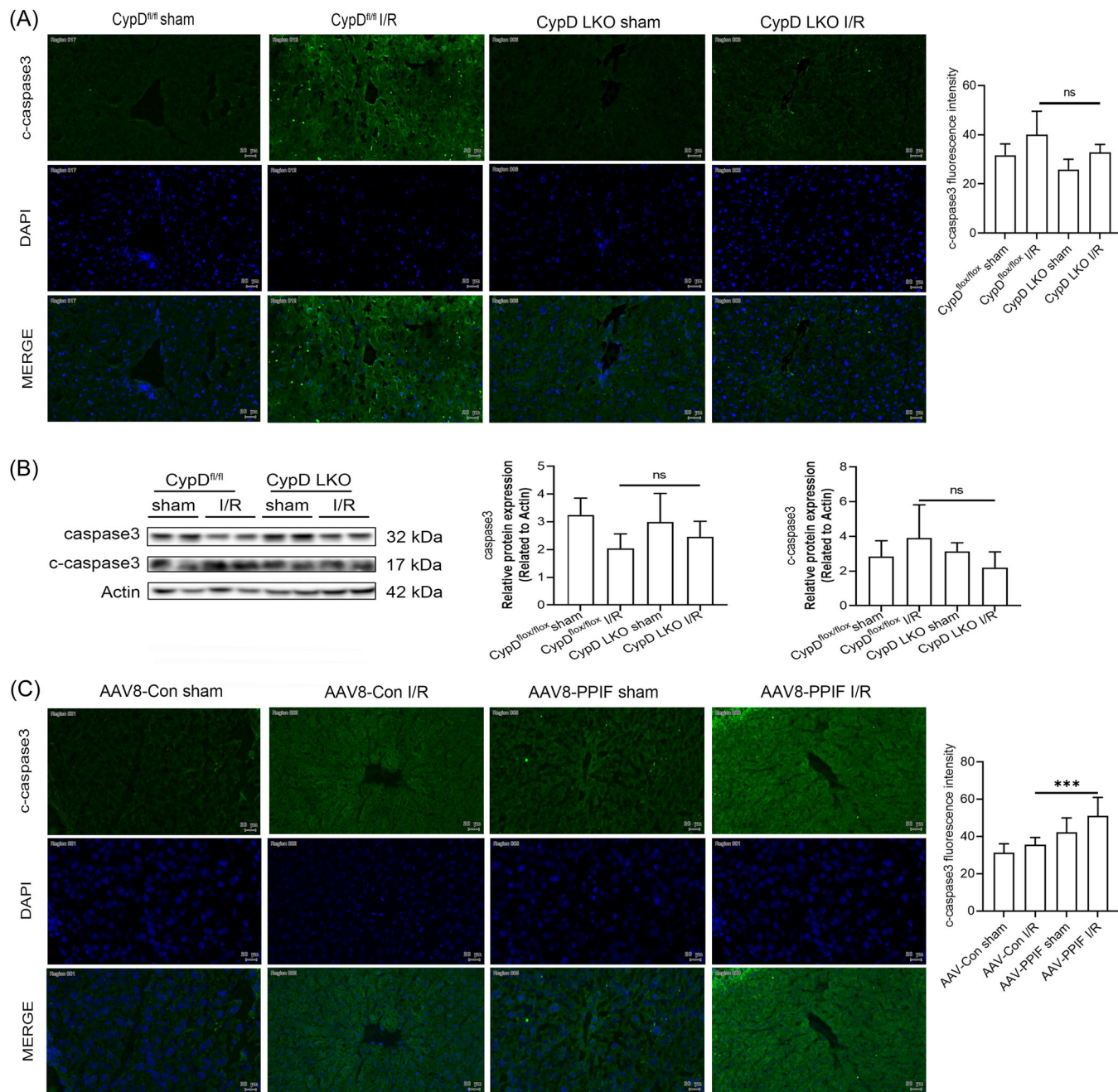


FIGURE 3 The effect of CypD on hepatocyte apoptosis in liver I/R injury. (A) The immunofluorescence of cleaved caspase-3 (fluorescent green) to measure the level of apoptosis in CypD^{fl/fl} group and CypD LKO group mice. Scale bar = 20 μ m ($n = 3$ per group). (B) Protein expression levels of apoptosis indices in liver tissue. (C) The immunofluorescence of cleaved caspase-3 (fluorescent green) to measure the level of apoptosis in AAV8-Con group and AAV8-PPIF group mice. Scale bar = 20 μ m ($n = 3$ per group). CypD, cyclophilin D; CypD LKO, liver-specific CypD knockout; I/R, ischemia/reperfusion; PPIF, peptidyl prolyl isomerase F.

FIGURE 2 After I/R surgery, ROS production and TUNEL in mouse liver. (A) Generation and distribution of ROS in the CypD^{fl/fl} group and CypD LKO group mice. Scale bar = 100 μ m ($n = 3$ per group). (B) Generation and distribution of ROS in AAV8-Con group and AAV8-PPIF group mice. Scale bar = 100 μ m ($n = 3$ per group). (C) TUNEL staining in liver tissues of CypD^{fl/fl} group and CypD LKO group mice. Scale bar = 50 μ m ($n = 3$ per group). (D) TUNEL staining in liver tissues of AAV8-Con group and AAV8-PPIF group mice. Scale bar = 50 μ m ($n = 3$ per group). CypD, cyclophilin D; CypD LKO, liver-specific CypD knockout; I/R, ischemia/reperfusion; PPIF, peptidyl prolyl isomerase F; ROS, reactive oxygen species; TUNEL, transferase dUTP nick-end labeling.

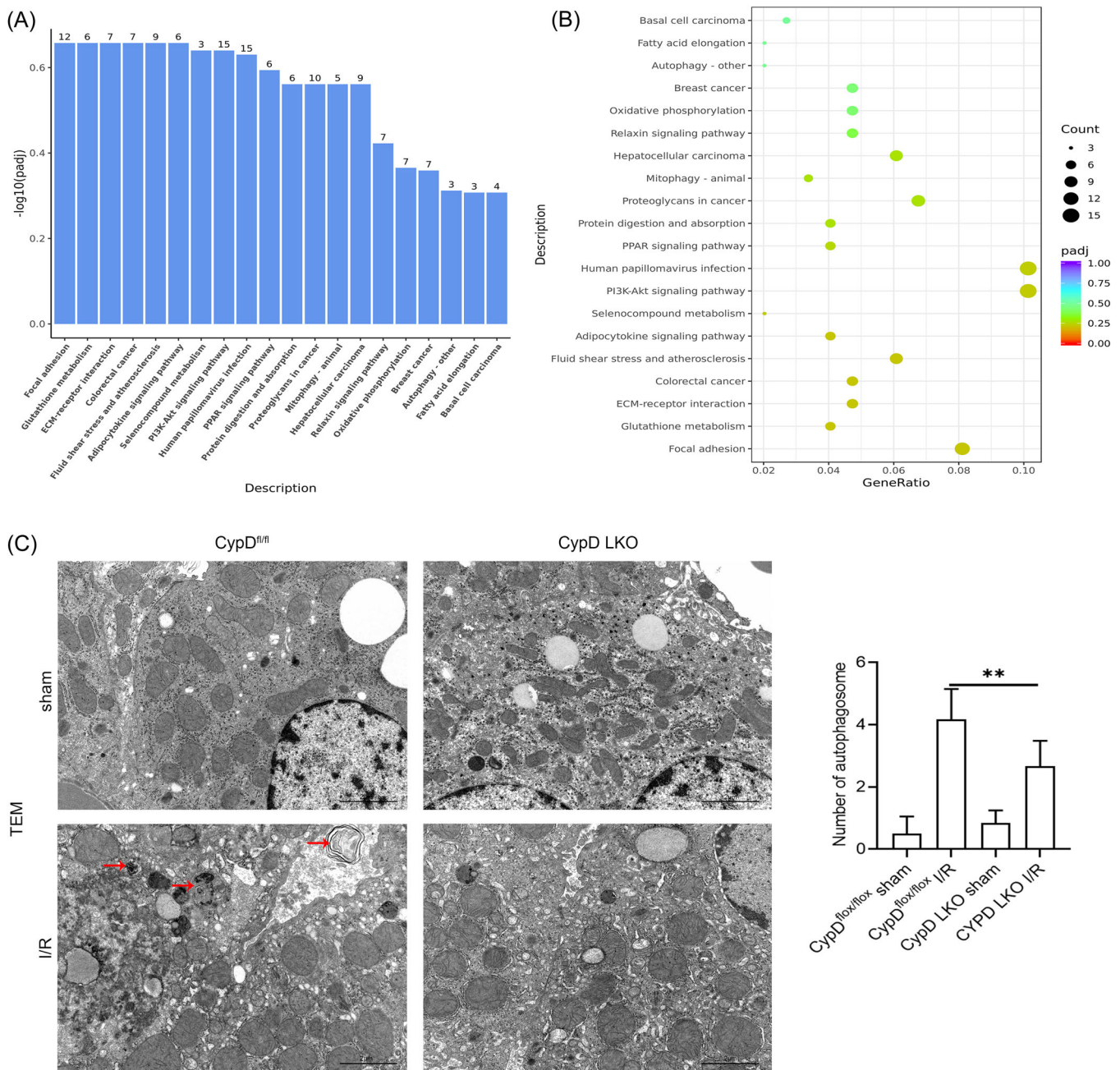


FIGURE 4 CypD participated in autophagic cell death in hepatic I/R injury. (A, B) Histogram and scatter plots of KEGG enrichment analysis of the 20 most significantly differential pathways between the CypD^{fl/fl} I/R group and the CypD LKO I/R group ($n = 3$ per group). (C) TEM was used to observe the quality of mitochondria and determine the number of autophagic vacuoles. Scale bar = 2 μm . CypD, cyclophilin D; CypD LKO, liver-specific CypD knockout; I/R, ischemia/reperfusion; KEGG, Kyoto Encyclopedia of Genes and Genomes; PPIF, peptidyl prolyl isomerase F; TEM, transmission electron microscopy.

circumstances. However, beyond this range, autophagy eventually leads to apoptotic cell death. From the enrichment analysis of KEGG pathways in RNA-seq, it can be observed that there is a significant difference in autophagy between the CypD^{fl/fl} I/R group and the CypD LKO I/R group. Furthermore, TEM results also revealed reduced autophagosomes and lysosomes in the CypD LKO group with less mitochondrial damage than in the control group with liver I/R injury. Damaged and

dysfunctional mitochondria can be selectively removed through autophagy, termed mitochondrial autophagy (mitophagy), which is an important process to maintain the mass of mitochondria.³³ The expression of the mitophagy-related protein TOMM20 was augmented in the CypD LKO group with I/R injury compared with the CypD^{fl/fl} control group. Our findings provide evidence that CypD is a pivotal regulator in the autophagic cell death pathway of liver I/R injury. Beclin1 is a novel

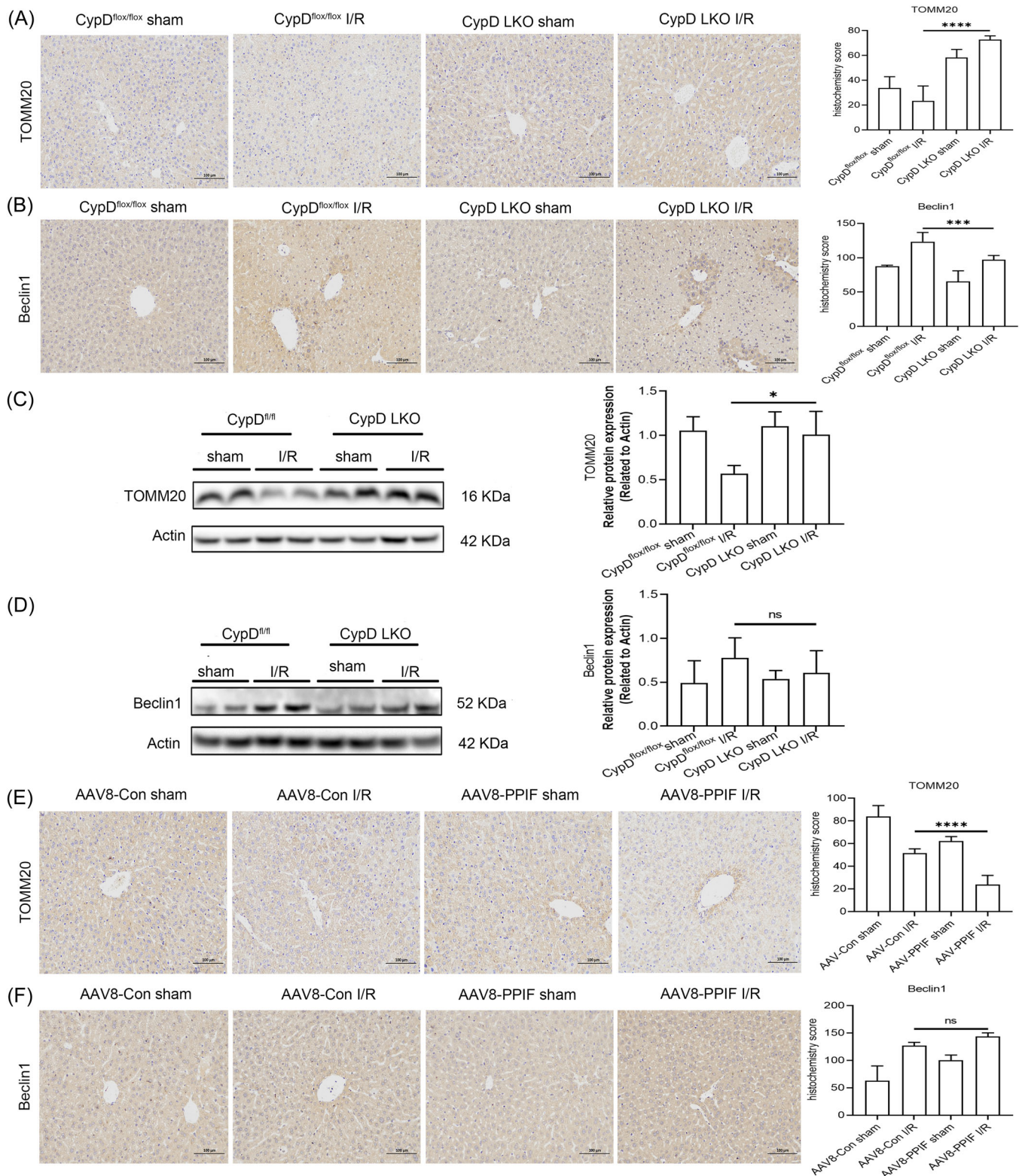


FIGURE 5 Effects of upregulation and downregulation of CypD on autophagy in mice with liver I/R injury. (A) Immunohistochemical staining of TOMM20 in liver-specific CypD knockout live tissue. Scale bar = 100 μ m ($n = 3$ per group). (B) Immunohistochemical staining of Beclin1 in liver-specific CypD knockout live tissue. Scale bar = 100 μ m ($n = 3$ per group). (C) Protein expression of TOMM20 in liver-specific CypD knockout live tissue. (D) Protein expression of Beclin1 in liver-specific CypD knockout live tissue. (E) Immunohistochemical staining of TOMM20 in the livers of AAV8-PPIF-overexpressing mice. Scale bar = 100 μ m ($n = 3$ per group). (F) Immunohistochemical staining of Beclin1 in the livers of AAV8-PPIF-overexpressing mice. Scale bar = 100 μ m ($n = 3$ per group). CypD, cyclophilin D; I/R, ischemia/reperfusion; PPIF, peptidyl prolyl isomerase F.

substrate that regulates autophagosome formation. Recently, accumulated evidence has suggested that Beclin1 interacts with autophagic cell death and apoptotic cell death pathways.^{34,35} Correspondingly, Beclin1 was significantly downregulated in the CypD LKO I/R group but increased in CypD-overexpressing mice.

Taken together, these data indicate that liver-specific knockout of CypD can reduce liver tissue injury and hepatocyte necrosis in I/R of the liver by alleviating apoptosis and autophagy. In addition, we discussed the essential role of caspase-3 and Beclin1 in the crosstalk between apoptotic and autophagic cell death in CypD knockout and overexpression mice of I/R. However, there are still some deficiencies in this study. First, AAV8-PPIF was injected into the tail vein as the overexpression model, and the knockout model was the CypD LKO gene model, which could not exclude the influence of the overall factors. In addition, how CypD regulates the opening of mPTP still needs further exploration. Furthermore, the accurate distinction of different cell death forms regulated by CypD should be studied in vitro. Nevertheless, the therapeutic strategy to target CypD could become an effective method for mitochondrial quality control and liver protection during I/R injury.

AUTHOR CONTRIBUTIONS

Study conception, design, and experimentation were handled by Mengjiao Yang, Siying Li, and Yongfeng Song. The experiment and data analysis were conducted by Zhihui Wang, Jin Xie, and Md. Reyad-ul-Ferdous. The manuscript draft was completed by Mengjiao Yang. The manuscript was reviewed and revised by all authors and obtained approval for submission.

ACKNOWLEDGMENTS

This work was supported by the National Natural Science Foundation of China (82270922), Shandong Provincial Natural Science Foundation (ZR2020ZD14), National Key Research and Development Program of China (2022YFA0806100) and independently cultivates innovation team program of Jinan, China (2021GXRC048).

CONFLICT OF INTEREST STATEMENT

The authors declare no conflict of interest. Professor Yongfeng Song is a member of Chronic Diseases and Translational Medicine editorial board and is not involved in the peer review process of this article.

DATA AVAILABILITY STATEMENT

Data sharing not applicable to this article as no datasets were generated or analyzed during the current study.

ETHICS STATEMENT

The Research Ethics Committee of Shandong Provincial Hospital approved all procedures (No. 2022-047).

ORCID

Siying Li  <http://orcid.org/0000-0001-6906-8394>

REFERENCES

1. Bi J, Zhang J, Ren Y, et al. Irisin alleviates liver ischemia-reperfusion injury by inhibiting excessive mitochondrial fission, promoting mitochondrial biogenesis and decreasing oxidative stress. *Redox Biol.* 2019;20:296-306. doi:10.1016/j.redox.2018.10.019
2. Pan Y, Wang X, Liu X, Shen L, Chen Q, Shu Q. Targeting ferroptosis as a promising therapeutic strategy for ischemia-reperfusion injury. *Antioxidants.* 2022;11(11):2196. doi:10.3390/antiox11112196
3. Hu C, Zhao L, Zhang F, Li L. Regulation of autophagy protects against liver injury in liver surgery-induced ischaemia/reperfusion. *J Cell Mol Med.* 2021;25(21):9905-9917. doi:10.1111/jcmm.16943
4. Elias-Miró M, Jiménez-Castro MB, Rodés J, Peralta C. Current knowledge on oxidative stress in hepatic ischemia/reperfusion. *Free Radic Res.* 2013;47(8):555-568. doi:10.3109/10715762.2013.811721
5. Zhai Y, Petrowsky H, Hong JC, Busuttill RW, Kupiec-Weglinski JW. Ischaemia-reperfusion injury in liver transplantation—from bench to bedside. *Nat Rev Gastroenterol Hepatol.* 2013;10(2):79-89. doi:10.1038/nrgastro.2012.225
6. Kalogeris T, Baines CP, Krenz M, et al. Cell biology of ischemia/reperfusion injury. *Int Rev Cell Mol Biol.* 2012;298:229-317. doi:10.1016/b978-0-12-394309-5.00006-7
7. Mansouri A, Gattolliat CH, Asselah T. Mitochondrial dysfunction and signaling in chronic liver diseases. *Gastroenterology.* 2018;155(3):629-647. doi:10.1053/j.gastro.2018.06.083
8. Kalogeris T, Baines CP, Krenz M, et al. Ischemia/Reperfusion. *Compr Physiol.* 2016;7(1):113-170. doi:10.1002/cphy.c160006
9. Lesnefsky EJ, Chen Q, Tandler B, Hoppel CL. Mitochondrial dysfunction and myocardial ischemia-reperfusion: implications for novel therapies. *Annu Rev Pharmacol Toxicol.* 2017;57:535-565. doi:10.1146/annurev-pharmtox-010715-103335
10. Peralta C, Jiménez-Castro MB, Gracia-Sancho J. Hepatic ischemia and reperfusion injury: effects on the liver sinusoidal milieu. *J Hepatol.* 2013;59(5):1094-1106. doi:10.1016/j.jhep.2013.06.017
11. Li J, Yan Z, Fang Q. A mechanism study underlying the protective effects of cyclosporine-A on lung ischemia-reperfusion injury. *Pharmacology.* 2017;100(1-2):83-90. doi:10.1159/000458760
12. Lin HC, Lee TK, Tsai CC, Lai IR, Lu KS. Ischemic postconditioning protects liver from ischemia-reperfusion injury by modulating mitochondrial permeability transition. *Transplantation.* 2012;93(3):265-271. doi:10.1097/TP.0b013e31823ef335
13. Giorgio V, Soriano ME, Basso E, et al. Cyclophilin D in mitochondrial pathophysiology. *Biochim Biophys Acta.* 2010;1797(6-7):1113-1118. doi:10.1016/j.bbabo.2009.12.006
14. Fayaz SM, Kumar VS, Rajanikant GK. Necroptosis: who knew there were so many interesting ways to die? *CNS Neurol Disord Drug Targets.* 2014;13(1):42-51. doi:10.2174/18715273113126660189
15. Fayaz S, Raj Y, Krishnamurthy R. CypD: the key to the death door. *CNS Neurol Disord Drug Targets.* 2015;14(5):654-663. doi:10.2174/1871527314666150429113239
16. Li X, Yang M, Sun H, et al. Liver cyclophilin D deficiency inhibits the progression of early NASH by ameliorating steatosis and inflammation. *Biochem Biophys Res Commun.* 2022;594:168-176. doi:10.1016/j.bbrc.2022.01.059
17. Zheng J, Chen L, Lu T, et al. MSCs ameliorate hepatocellular apoptosis mediated by PINK1-dependent mitophagy in liver ischemia/reperfusion injury through AMPK α activation. *Cell Death Dis.* 2020;11(4):256. doi:10.1038/s41419-020-2424-1
18. Lin J, Huang H, Yang S, et al. The effect of Ginsenoside Rg1 in hepatic ischemia reperfusion (I/R) injury ameliorates

- ischemia-reperfusion-induced liver injury by inhibiting apoptosis. *Biomed Pharmacother.* 2020;129:110398. doi:10.1016/j.biopha.2020.110398
19. Go KL, Lee S, Zendejas I, Behrns KE, Kim JS. Mitochondrial dysfunction and autophagy in hepatic ischemia/reperfusion injury. *BioMed Res Int.* 2015;2015:1-14. doi:10.1155/2015/183469
 20. Nguyen TT, Stevens MV, Kohr M, Steenbergen C, Sack MN, Murphy E. Cysteine 203 of cyclophilin D is critical for cyclophilin D activation of the mitochondrial permeability transition pore. *J Biol Chem.* 2011;286(46):40184-40192. doi:10.1074/jbc.M111.243469
 21. Xu T, Ding W, Ao X, et al. ARC regulates programmed necrosis and myocardial ischemia/reperfusion injury through the inhibition of mPTP opening. *Redox Biol.* 2019;20:414-426. doi:10.1016/j.redox.2018.10.023
 22. Cai LL, Xu HT, Wang QL, et al. EP4 activation ameliorates liver ischemia/reperfusion injury via ERK1/2-GSK3 β -dependent MPTP inhibition. *Int J Mol Med.* 2020;45(6):1825-1837. doi:10.3892/ijmm.2020.4544
 23. Wang X, Du H, Shao S, et al. Cyclophilin D deficiency attenuates mitochondrial perturbation and ameliorates hepatic steatosis. *Hepatology.* 2018;68(1):62-77. doi:10.1002/hep.29788
 24. Bonora M, Patergnani S, Ramaccini D, et al. Physiopathology of the permeability transition pore: molecular mechanisms in human pathology. *Biomolecules.* 2020;10(7):998. doi:10.3390/biom10070998
 25. Zhang L, Liu Y, Zhou R, He B, Wang W, Zhang B. Cyclophilin D: guardian or executioner for tumor cells? *Front Oncol.* 2022;12:939588. doi:10.3389/fonc.2022.939588
 26. Mammucari C, Rizzuto R. Signaling pathways in mitochondrial dysfunction and aging. *Mech Ageing Dev.* 2010;131(7-8):536-543. doi:10.1016/j.mad.2010.07.003
 27. Saxton NE, Barclay JL, Clouston AD, Fawcett J. Cyclosporin A pretreatment in a rat model of warm ischaemia/reperfusion injury. *J Hepatol.* 2002;36(2):241-247. doi:10.1016/s0168-8278(01)00248-3
 28. Skinner S, Solania A, Wolan D, Cohen M, Ryan T, Hepple R. Mitochondrial permeability transition causes mitochondrial reactive oxygen species- and caspase 3-dependent atrophy of single adult mouse skeletal muscle fibers. *Cells.* 2021;10(10):2586. doi:10.3390/cells10102586
 29. Mizushima N, Komatsu M. Autophagy: renovation of cells and tissues. *Cell.* 2011;147(4):728-741. doi:10.1016/j.cell.2011.10.026
 30. Lőrincz P, Juhász G. Autophagosome-lysosome fusion. *J Mol Biol.* 2020;432(8):2462-2482. doi:10.1016/j.jmb.2019.10.028
 31. Kong W, Li W, Bai C, Dong Y, Wu Y, An W. Augmenter of liver regeneration-mediated mitophagy protects against hepatic ischemia/reperfusion injury. *Am J Transplant.* 2022;22(1):130-143. doi:10.1111/ajt.16757
 32. Ma Y, Jiao Z, Liu X, et al. Protective effect of adipose-derived stromal cell-secretome attenuate autophagy induced by liver ischemia-reperfusion and partial hepatectomy. *Stem Cell Res Ther.* 2022;13(1):427. doi:10.1186/s13287-022-03109-2
 33. Lee J, Giordano S, Zhang J. Autophagy, mitochondria and oxidative stress: cross-talk and redox signalling. *Biochem J.* 2012;441(2):523-540. doi:10.1042/bj20111451
 34. Kang R, Zeh HJ, Lotze MT, Tang D. The Beclin 1 network regulates autophagy and apoptosis. *Cell Death Differ.* 2011;18(4):571-580. doi:10.1038/cdd.2010.191
 35. Prerna K, Dubey VK. Beclin1-mediated interplay between autophagy and apoptosis: new understanding. *Int J Biol Macromol.* 2022;204:258-273. doi:10.1016/j.ijbiomac.2022.02.005

SUPPORTING INFORMATION

Additional supporting information can be found online in the Supporting Information section at the end of this article.

How to cite this article: Yang M, Wang Z, Xie J, et al. Cyclophilin D as a potential therapeutic target of liver ischemia/reperfusion injury by mediating crosstalk between apoptosis and autophagy. *Chronic Dis Transl Med.* 2023;9: 238-249. doi:10.1002/cdt3.78